Poly(basic red 9) doped functionalized multi-walled carbon nanotubes as composite films for neurotransmitters biosensors

Ying Li [a], M. Ajmal Ali [b], Shen-Ming Chen [a,b,∗], Shin-Ying Yang [a], Bih-Show Lou [c,∗∗], Fahad M.A. Al-Hemaid [b]

[a] Department of Chemical Engineering and Biotechnology, National Taipei University of Technology, No. 1, Section 3, Chung-Hsiao East Road, Taipei 106, Taiwan, ROC
[b] Department of Botany and Microbiology, College of Science, King Saud University, Riyadh 11451, Saudi Arabia
[c] Chemistry Division, Center for General Education, Chang Gung University, 259, Wen-Hwa 1st Road, Kwei-Shan, Tao-Yuan 333, Taiwan, ROC

ABSTRACT

This paper discusses the electrochemical polymerization of basic dye films, which are composed of basic red 9 (BR9), on various electrodes and the enhancement of the electropolymerization by functionalized multiwall carbon nanotubes (f-MWCNTs) modification of the electrode surface. The presence of f-MWCNTs enhances the surface coverage (Γ) and stability. Poly(BR9) films were electrocatalytically active for epinephrine and serotonin oxidation. The electrocatalytic oxidation current developed from the anodic peak of the redox couple. Electrochemical impedance spectroscopy (EIS) was applied to monitor the whole process of the electrode modification. EIS can provide useful information regarding the impedance changes on the electrode surface between each step. We studied the surface morphology of the composite film using scanning electron microscopy (SEM) and atomic force microscopy (AFM), which revealed that BR9 is doped on f-MWCNTs. Cyclic voltammetry (CV) was used for the measurement of the electroanalytical properties of the analytes. The sensitivity values for the f-MWCNTs/BR9 composite film were higher than the poly(BR9) and f-MWCNTs composite film. Finally, differential pulse voltammetry (DPV) was used for the detection of a mixture of analytes at the f-MWCNTs/BR9 composite film. We simulated a more complex system with both serotonin and epinephrine present simultaneously. This system also exhibited oxidation peaks for serotonin in bovine calf serum (BCS) and epinephrine injection for real samples determination at pH 7.0 at the f-MWCNTs/BR9 composite film.

© 2014 Elsevier B.V. All rights reserved.

1. Introduction

C.I. basic red 9 (BR9), a triarylmethane dye, was selected as the model compound to determine the interactions between dye and surfactant molecules. Other triamino derivatives of triphenylmethane dyes are produced by connecting the various functional compounds to the amino groups on the triphenylmethane. BR9 is also commonly used in the textile, leather, paper and ink industries [1]. Azo dyes, such as BR9 (contain —N=N— bonds), are resistant to

biodegradation under aerobic conditions, whereas anaerobic treatment is applied successfully [2].

Electropolymerization of anilines linked with triarylamines causes polymerization of the three branches [3]. Several reports reveal that the polymerization a triphenylmethane derivative, fuchsin acid, a molecule that has three branched monomers, leads to a dendritic polymer [4]. Varieties of applications of carbon nanotubes (CNT) with dye were previously reported [5–7]. Although the electrocatalytic activity of the conjugated polymers and CNTs matrices individually exhibit excellent results, certain properties, such as the mechanical stability, sensitivity for different techniques and electrocatalysis of multiple compounds, are found to be poor.

Epinephrine (EP) is an important catecholamine neurotransmitter in the mammalian central nervous system and exists in the nervous tissue and body fluids as large organic cations [8]. EP plays an important role in the function of the central nervous, renal, hormonal, and cardiovascular systems [9]. The catecholamine drugs are used to treat hypertension, bronchial asthma, and organic heart

∗ Corresponding authors at: National Taipei University of Technology, Department of Chemical Engineering and Biotechnology, 1, Sec 3, Chung-Hsiao E Rd, Taipei 106, Taiwan, ROC. Tel.: +886 2270 17147; fax: +886 2270 25238.
∗∗ Corresponding author at: Chang Gung University, Chemistry Division, Center for General Education, 259, Wen-Hwa 1st Road, Kwei-Shan, Tao-Yuan 333, Taiwan, ROC. Tel: +886-2118800 5018; fax: +886-2118700.
E-mail addresses: smchen78@ms15.hinet.net (S.-M. Chen), blou@mail.cgu.edu.tw (B.-S. Lou).

disease and are used in cardiac surgery and myocardial infarction [10–12]. This compound controls the nervous system performance for a series of biological reactions and nervous chemical processes. Many diseases are related to changes of the EP concentration in living systems.

Serotonin (5-hydroxytryptamine, 5-HT) is a biogenic monoamine neurotransmitter that is synthesized both in the enteric nervous system and the central nervous system [13,14]. Serotonin is of enormous biological importance and is widely distributed in the central nervous system. A deficiency leads to mental disorders, such as Alzheimer's disease, infantile autism, mental retardation, sleep disorders and depression [15–17]. Electrochemical analysis at unmodified electrodes has limitations because of the overlapping of the oxidation potentials of biochemical compounds, and hence, often suffers from a pronounced fouling effect along with poor selectivity and reproducibility [18,19]. In the past, several modified electrodes were used for the simultaneous determination of neurotransmitters [20,21].

The quantitative determination of EP and serotonin concentrations is also helpful for developing nerve physiology, clinical diagnosis of some diseases and controlling medicine in pharmacological research [22]. The oxidation of these compounds is interesting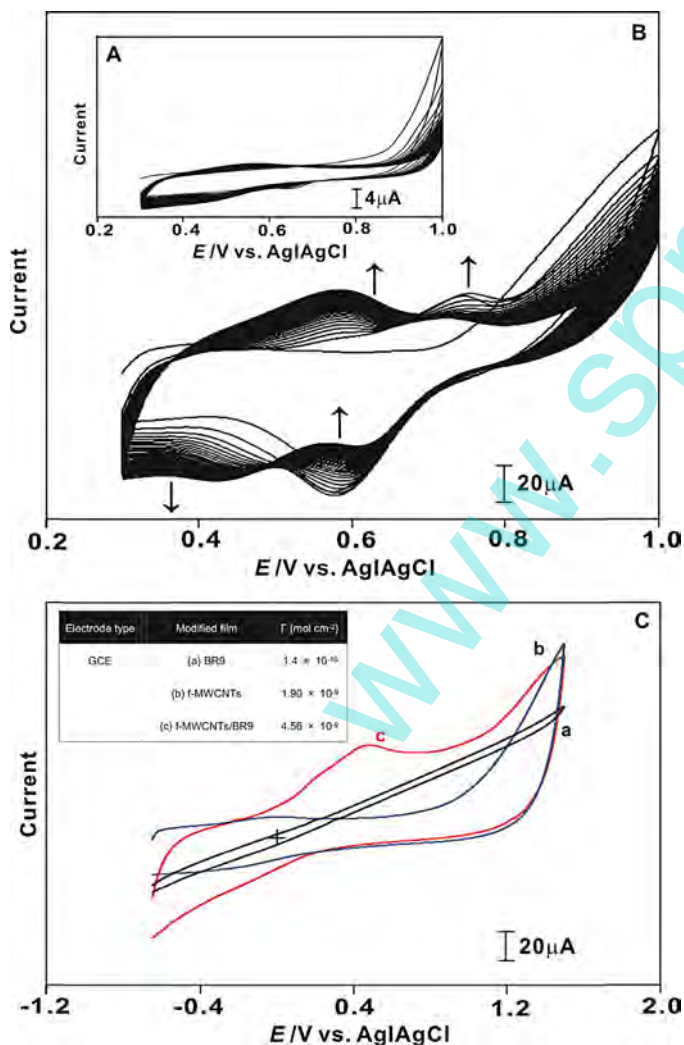 because this process occurs in the human body. Due to their crucial role in neurochemistry and industrial applications, several traditional methods have been used for their determination. Therefore, it is important to examine the electrochemical behavior and to develop a quantitative method for studying the concentrations in body fluids [23]. Among these methods, electrochemical methods have more advantages over the others in sensing neurotransmitters present in living organisms [24].

This paper discusses the electrochemical polymerization of basic dye films composed of BR9 on various electrodes and the enhancement of the electropolymerization by functionalized multiwall carbon nanotubes f-MWCNTs modification of the electrode surface. Two-layer modified electrodes were prepared from poly(BR9) and f-MWCNTs composite films. Poly(BR9) films were electrocatalytically active for epinephrine and serotonin oxidation. The electrocatalytic oxidation current was observed to develop from the anodic peak of the redox couple.

2. Experimental

2.1. Materials

Multi-walled carbon nanotubes (Aldrich) were used as received. C.I. BR9 (parafuchsin) was obtained from Fluka. EP, serotonin (5-HT), ascorbic acid (AA), uric acid (UA) and bovine calf serum (BCS) were obtained from Sigma. The EP injection was from Adrenalin®. All other chemicals were of analytical grade and were used without further purification Phosphate buffered saline (PBS, 0.1 M) and pH 1.0 H_2SO_4 solutions were used as the supporting electrolyte. Aqueous solutions were prepared using double-distilled deionized water and were de-aerated by purging with high purity nitrogen gas for approximately 20 min prior to performing the electrochemical experiments. In addition, a continuous flow of nitrogen over the aqueous solution was maintained during the measurements. Indium tin oxide (ITO) ($7\,\Omega\,cm^{-2}$) was purchased from Merck Display Technologies (MDT) Ltd. (Taiwan).

2.2. Apparatus

Cyclic voltammetry (CV) and linear sweep voltammetry (LSV) were performed using a CHI-1205B, and differential pulse voltammetry (DPV) was conducted using a CHI-900 and CHI-410
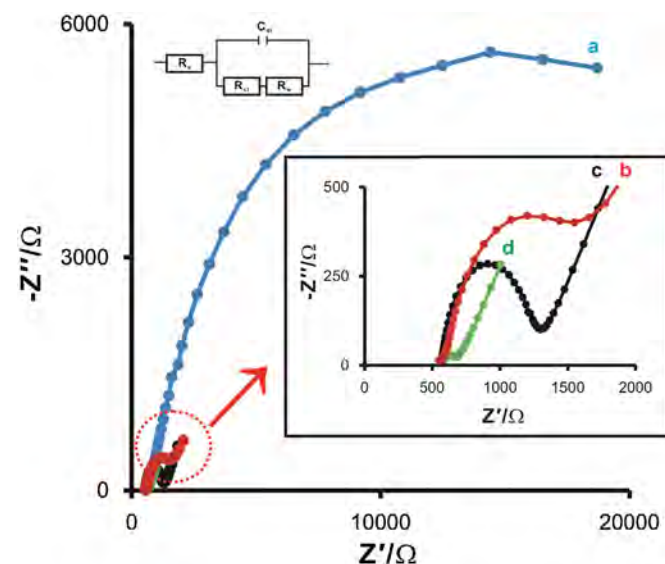

Fig. 1. Repetitive CVs of (A) BR9 and (B) f-MWCNTs/BR9 films from 5 mM BR9 in pH 1.0 H_2SO_4 buffer, scan rate at $100\,mV\,s^{-1}$. (C) Comparison of CVs of (a) BR9, (b) f-MWCNTs and (c) f-MWCNTs/BR9 films on GCE in pH 7.0 PBS buffer, scan rate at $100\,mV\,s^{-1}$.

Fig. 2. Electrochemical impedance spectra (EIS) of (a) only BR9, (b) f-MWCNTs/BR9, (c) bare GCE and (d) f-MWCNTs in pH 7.0 PBS containing 5×10^{-3} M $[Fe(CN)_6]^{-3/-4}$ (Amplitude: 5 mV).

potentiostat. A conventional three-electrode cell assembly consisting of an Ag/AgCl reference electrode and a Pt wire counter electrode was used for the electrochemical measurements. The working electrode was a glassy carbon electrode (GCE; area 0.07 cm^2). The potentials were reported versus the Ag/AgCl reference electrode. The morphologies of the films were examined using scanning electron microscopy (SEM) (Hitachi S-3000H) and atomic force microscopy (AFM) (Being Nano-Instruments CSPM5000). Electrochemical impedance spectroscopy (EIS) measurements were performed using an IM6ex Zahner instrument (Kroanch, Germany). All experiments were performed at room temperature (≈25 °C).

2.3. Preparation of composite films

The produced *f*-MWCNTs were suspended in a concentrated sulfuric acid–nitric acid mixture (3:1 v/v) and sonicated in a sonication bath for 2 h. A nanotube mat was obtained after filtration using a 0.45 mm hydrophilized PTFE membrane and washing with deionized water until no acid was detected, followed by drying under vacuum [25]. The obtained 10 mg *f*-MWCNTs in 10 mL water was ultrasonicated for 6 h to obtain a uniform dispersion. This functionalization process of *f*-MWCNTs was performed to obtain a hydrophilic nature for the homogeneous dispersion. This process not only converts *f*-MWCNTs to hydrophilic nature but also helps to breakdown larger bundles of *f*-MWCNTs into smaller bundles [26].
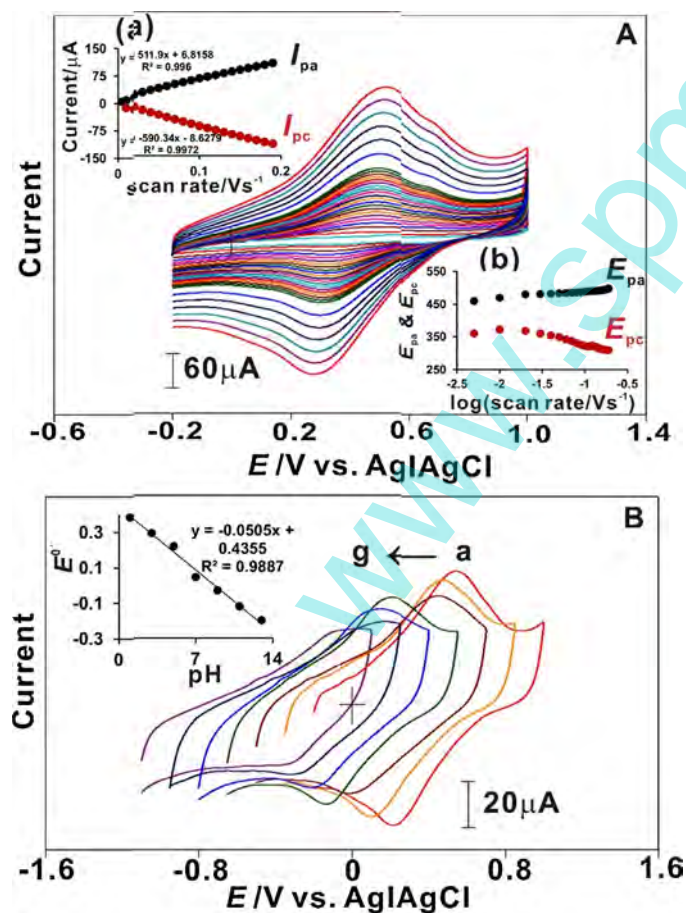

Fig. 3. (A) Cyclic voltammograms of pH 1.0 H$_2$SO$_4$ at *f*-MWCNTs/BR9 electrodes at different scan rates from 5 mV s^{-1} to 500 mV s^{-1}. Calibration curve of (a) I_{pa} and I_{pc} vs. scan rate and (b) E_{pa} and E_{pc} vs. log(scan rate). (B) Cyclic voltammograms of the *f*-MWCNTs/BR9 film transferred to various pH solutions (a) 1; (b) 3; (c) 5; (d) 7; (e) 9; (f) 11; and (g) 13. The inset displays the formal $E^{0'}$ vs. pH.

Prior to modification, the glassy carbon electrode (GCE) was polished with 0.05 μm alumina on Buehler felt pads and then ultrasonically cleaned for a minute in water. Finally, the electrode was washed thoroughly with double-deionized water and dried at room temperature. The cleaned glassy carbon electrode was coated with 2 μL of *f*-MWCNTs, and the solvent was allowed to evaporate at room temperature. The electropolymerization of BR9 was performed by electrochemical oxidation of BR9 (5 mM) on the *f*-MWCNT modified glassy carbon electrode in pH 1.0 aqueous H$_2$SO$_4$ solution vs. pH 1.0 H$_2$SO$_4$ solutions. It was performed by consecutive CVs over a suitable potential range of 0.3 to 1.0 V with a scan rate = 100 mV s^{-1}. The optimization of the poly-BR9 growth potential has been determined by various studies with different electropolymerization potentials.

3. Results and discussion

3.1. Electrochemical characterizations of f-MWCNTs/BR9 composite film

The BR9 adhered on a GCE by *f*-MWCNTs. The former composite film was prepared using electrochemical oxidation with an anodic wave current occurring between the potentials of 0.3 to 1.0 V. Fig. 1(A) displays the poly-BR9 growth by cyclic voltammogram current, exhibiting a redox couple with a formal potential of $E^{0'}$ = 0.52 V (vs. Ag|AgCl). The increase of the peak current at the redox couple indicates that film formation occurred. The second type of electrochemical film formation arising from the adherence of BR9 on an *f*-MWCNTs-modified glassy carbon electrode was performed using consecutive CV between the same conditions. Fig. 1(B) displays the larger growth of the peak current than poly-(BR9) film. The growth in the cyclic voltammetric current showed that the redox couple occurred at a formal potential of $E^{0'}$ = 0.50 V (vs. Ag|AgCl). The more rapidly increased and larger magnitude of the peak current indicates that film formation occurred, and the film was enhanced by the modified electrode surface and the *f*-MWCNTs. The poly(BR9) films could also be synthesized in strong acidic aqueous solutions using consecutive CV on ITO electrodes that had been modified by including *f*-MWCNTs on the electrode surface.

In the following experiments, each newly prepared film on a glassy carbon electrode was washed carefully in deionized water to remove the loosely bounded BR9 on the modified glassy carbon electrode. The film was subsequently transferred to pH 7.0 PBS and pH 1.0 aqueous H$_2$SO$_4$ solutions vs. pH 1.0 H$_2$SO$_4$ solutions for further electrochemical characterizations. These optimized pH solutions have been chosen to maintain the higher stability (pH = 7.0).

Fig. 1(C) displays (a) poly(BR9), (b) *f*-MWCNTs and (c) *f*-MWCNTs/BR9 films. The corresponding cyclic voltammograms were measured at a 100 mV s^{-1} scan rate in the potential range of −0.65 to 1.5 V. From Fig. 1(C), the defined oxidation peak was observed at 0.47 V (vs. Ag|AgCl) for *f*-MWCNTs/BR9 (curve *c*) films. However, there were no peaks for the *f*-MWCNTs (curve *b*) and BR9 (curve *a*) films. Similar results have been observed at ITO electrodes (figure not shown). Moreover, several studies have reported nearly reversible redox peaks for fuchsin acid-Nafion films at $E^{0'}$ = 0.66 V vs. SCE in pH 1.5 [4]. A comparison of curve (*a*) and curve (*c*) shows the catalytic effect on the BR9 redox peak currents in the presence of *f*-MWCNTs. Further, it has been observed that the presence of *f*-MWCNTs increases the overall background current, which is similar to that of previous studies [27,28].

These above results show that BR9 exhibits reversible redox peaks only in the presence of *f*-MWCNTs at various electrodes. The surface coverage (Γ) values of different composite films have been

calculated and are given in the Fig. 1(C) inset. The Γ value was applied in the equation: $\Gamma = Q/nFA$, where Q is the charge, n is the number of electrons involved, F is the Faraday current, A is the electrode area, and the number of electrons transferred is two. We can note the enhanced Γ of BR9 in the f-MWCNTs modified electrode. These values indicate that the presence of f-MWCNTs increased the surface area of the electrode, which in turn has increased the Γ of BR9. The calculated values from the same table show that the increase in the Γ of BR9 in the presence of f-MWCNTs film is 4.42×10^{-9} mol cm^{-2}.

3.2. Electrochemical impedance spectroscopy (EIS) of analysis

EIS was applied to monitor the process of the electrode modification. EIS can give useful information of the impedance changes on the electrode surface between each step. Fig. 2 shows the results of EIS for a bare GCE and three other modified electrodes in the presence of equimolar 5 mM [Fe(CN)$_6$]$^{3-/4-}$ in pH 7.0 PBS. The EIS includes a semicircular part and a linear part. The semicircular part at higher frequencies corresponds to the electron transfer limited process, and the diameter is equivalent to the electron transfer resistance (R_{ct}). The linear part at lower frequencies corresponds to the diffusion process. During the fabrication, significant differences were observed. The R_{ct} of a f-MWCNTs/GCE is 689 Ω (curve d). The R_{ct} of a bare GCE is 1368 Ω (curve c). When the GCE was modified with BR9, the R_{ct} value was increased markedly to 18,760 Ω (curve a). The EIS results for the electrode modified with the f-MWCNTs/BR9 are shown in curve b, and the R_{ct} was considerably decreased to 1549 Ω. These results confirmed that the f-MWCNTs/BR9 film was successfully immobilized on the GCE surface. From these observations, we can conclude that the f-MWCNTs were highly conductive and are expected to act as a good platform for sensing applications.

3.3. Different scan rate studies of composite films

Fig. 3(A) shows that the f-MWCNTs/BR9 film on a glassy carbon electrode had one chemically reversible redox couple at 0.40 V in the pH 1.0 aqueous H$_2$SO$_4$ solution vs. pH 1.0 H$_2$SO$_4$ solutions when CV was performed at different scan rates (5 to 500 mV s^{-1}). The anodic and cathodic peak currents of both the film redox couples increased linearly with the increase of scan rates. The inset calibration curve for the data in Fig. 3(A) displays (a) I_{pa} and I_{pc} vs. scan rate and (b) E_{pa} and E_{pc} vs. log(scan rate). The ratio of the I_{pa}/I_{pc} from the inset demonstrated that the redox process is not controlled by diffusion. This behavior occurs because of a reversible electron transfer process involving the poly(BR9) on the f-MWCNTs layer, with a proton exchange process occurring along with the electron transfer process. However, the ΔE_p of each scan rate reveals that the peak separation of the composite redox couple increases as the scan rate is increased.

3.4. pH influence on the composite films

Fig. 3(B) displays the cyclic voltammogram of f-MWCNTs/BR9 composite films on an electrode obtained in pH 1.0 aqueous H$_2$SO$_4$ solution vs. pH 1.0 H$_2$SO$_4$ solutions and transferred to various pH aqueous buffer solutions. The composite film is highly stable in the pH range between 1.0 and 13. The values of E_{pa} and E_{pc} depend on the pH value of the buffer solution. The inset in Fig. 3(B) displays the potential of f-MWCNTs/BR9 plotted over a pH range from 1.0 to 13. The response slope is −50 mV/pH, which is close to the Nernstian equation for an equal number of electrons and protons transferred [29,30]. The pH response results are due to the deprotonation of the nitrogen atom of poly(BR9) or the counter ion near the amine functional group. The values of $E^{0'}$, which depend on the pH, also show that the redox couple of the polymeric film includes
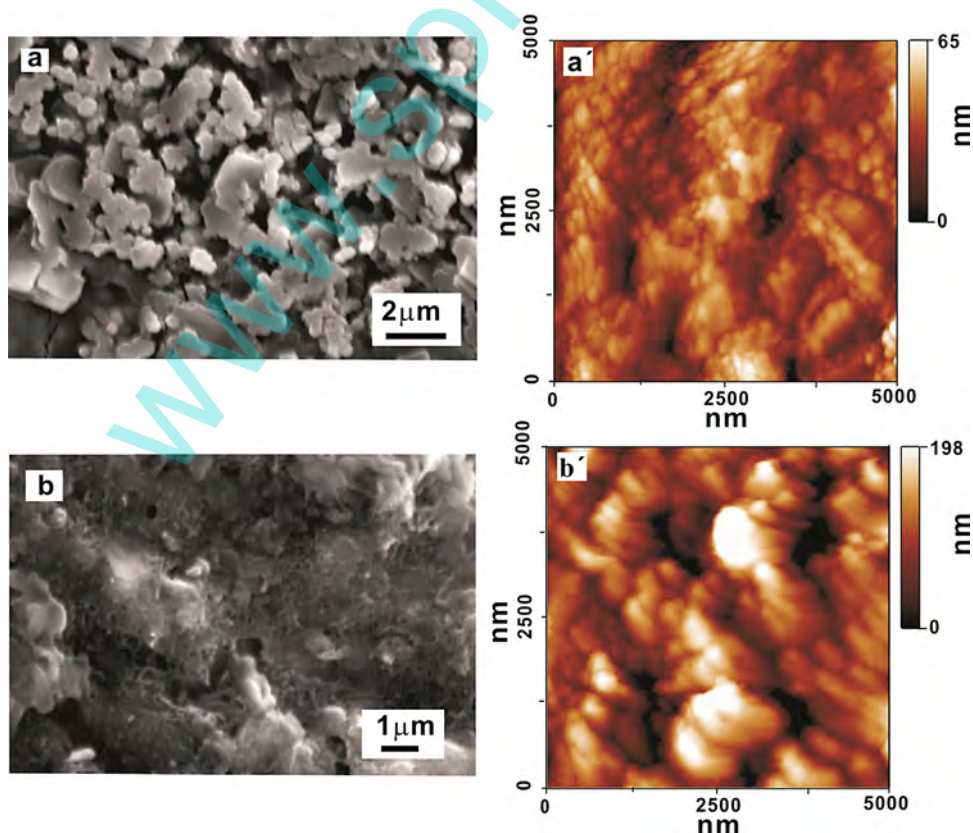

Fig. 4. SEM and AFM images of (a) (a′) BR9 and (b) (b′) f-MWCNTs/BR9 film on ITO electrode.

proton transfer in the reduction and oxidation processes. The chemical composition and possible electropolymerization of a poly(BR9) film is analogous to that of polyaniline and its analogues [31,32].

3.5. Morphological characterization of f-MWCNTs/BR9 film

Fig. 4 represents the top view SEM images of different films coated on ITO surfaces. Prior to modification, the ITO surfaces were cleaned and ultrasonicated in an acetone–water mixture for 15 min and then dried. Subsequently, the BR9 and f-MWCNTs/BR9 films were prepared on the ITO electrode. In Fig. 4, morphological differences among the films can be observed. The top views of the nano-structures (a) on the ITO electrode surface reveal uniform BR9 on the electrode. The f-MWCNTs/BR9 film in (b) displayed a BR9 coating over the entire f-MWCNT surface.

The surface morphologies of the electrodes were also examined using AFM. The AFM results provided comprehensive information about the surface morphology of the nanostructures on the ITO surface. The AFM images were collected over 5000×5000 nm surface areas and were used to determine the roughness average (sa), an expression of the surface roughness or texture that is typically used to describe a polished or machined metal surface, and the arithmetic average value of the departure (peaks and valleys) of the surface profile from the center-line through the sampling length. In addition, the BR9 and f-MWCNTs/BR9 films on the ITO electrode were characterized using AFM. From Fig. 4, it is apparent that there are morphological differences among the films. The top views of the nanostructures Fig. 4(a′) reveals uniformly deposited and homogeneously dispersed BR9 on the electrode. Nanostructures were present with an average height of 37.75 nm. The roughness average (sa) for the BR9 was 9.26 nm, and the root mean square roughness was 11.4 nm. The total surface area was 9262,283.51 (nm × nm). Fig. 4(b′) displays an image of the f-MWCNTs/BR9, which exhibited a roughness average (sa) and root mean square roughness of 36.7 nm and 45.3 nm, respectively. The average height and total surface area were 114.1 nm and 27,205,714.44 (nm × nm), respectively.

3.6. Electrocatalytic response of serotonin and epinephrine

Fig. 5(A) and (B) displays the electrocatalytic oxidation of serotonin and EP at f-MWCNTs/BR9 composite films with a scan rate of 100 mV s^{-1}. In all of the sections of Fig. 5, curve (a) was the f-MWCNTs/BR9 film in pH 7.0 PBS; curve (a′) and curve (b) were

bare glassy carbon electrode and f-MWCNTs/BR9 film at the highest concentrations of serotonin (5 mM) or epinephrine (2.67 mM). The CVs for f-MWCNTs/BR9 exhibit a reversible redox couple in the absence of serotonin and EP, and on the addition of analytes, a growth in the oxidation peak appeared at $E_{pa} = 0.55$ V for serotonin (Fig. 5A) and $E_{pa} = 0.41$ V for EP (Fig. 4B). The peak current shows that the electrocatalytic oxidation of both analytes takes place at the poly(BR9) redox couple. The inset of Fig. 5(A) and (B) displays (a) only BR9, (b) f-MWCNTs, and (c) f-MWCNTs/BR9 films at the highest concentrations of analytes. The f-MWCNTs/BR9 film has higher electrocatalytic activity for both serotonin and EP than for only BR9 and the f-MWCNTs films. The results were observed from the I_{pa} and E_{pa} values, where the increase in the peak current and lower over-potential are considered as electrocatalysis [33]. The sensitivity of the f-MWCNTs/BR9 film is higher for both analytes when compared with f-MWCNTs and only BR9 film. The overall view of the results clearly reveals that f-MWCNTs/BR9 is efficient for serotonin and EP detection.

3.7. Differential pulse voltammetry (DPV) of the mixture analytes at f-MWCNTs/BR9

The DPV values were recorded at a constant time interval of 2 min, with nitrogen purging performed prior to the start of each experiment. Fig. 6(A) serotonin and Fig. 6(B) EP display the f-MWCNTs/BR9 film in the presence of varying concentrations (a) 0; (b) 1.96×10^{-5} M; (c) 2.91×10^{-5} M; (d) 3.84×10^{-5} M; (e) 4.76×10^{-5} M; (f) 5.66×10^{-5} M; (g) 6.54×10^{-5} M; (h) 7.41×10^{-5} M; (i) 8.25×10^{-5} M of analyte. The peak currents for serotonin and EP increased linearly with the analyte concentration. These results demonstrate the calibration curves for the analyte, which are almost linear for a wide range of concentrations, as shown in the inset. The detection limits of the f-MWCNTs/BR9 film for serotonin and EP were 7.0×10^{-6} M and 9.0×10^{-6} M, which cover the concentration range found in physiological conditions. From the slopes of the linear calibration curves, the sensitivity of the f-MWCNTs/BR9 films and their correlation coefficients have been calculated in Table 1.

We simulated more complex system with both serotonin and EP present simultaneously. Fig. 6(C) displays the simultaneous change in the concentrations of the analyte mixture (serotonin 1.0×10^{-4} M with EP 1.0×10^{-3} M in pH 7.0 PBS) at the f-MWCNTs/BR9 film. The peak currents for the mixture analyte increased linearly with the analyte concentration. All of these

Table 1
Electroanalytical results for serotonin and EP present individually at the f-MWCNTs/BR9 using DPV.

Analytes	E_{pa} (mV)			I_{pa} (μA)	Concentration range (mM)		Detection limit (mM)	Sensitivity (μA mM^{-1} cm^{-2})
	Initial conc.	Final conc.	Difference		Low	High		
Serotonin	332.8	331.1	1.7	44.7	0.01	0.083	0.091	4684 [0.99]
EP	165.4	171.8	6.4	28.1	0.01	0.083	0.1	5214 [0.97]

Table 2
Experimental conditions and analytical parameters for serotonin and epinephrine determination using modified electrodes.

	Electrode	Technique	E_P (V) (Ag/AgCl)	Electrolyte	LOD (M)	Reference
Serotonin	GCE(ox)	SWAV	0.4	pH 7.0 PBS	3.0×10^{-8}	[34]
Serotonin	TPyP–3IP/FTO	CVs	0.21	pH 7.4 PBS	2.24×10^{-4}	[35]
Serotonin	GN-SPEs	CVs	0.28	pH 5.4 acetate	1.0×10^{-4}	[36]
EP			0.125	buffer	1.0×10^{-4}	
Serotonin	GNPs/GCE	SWV	0.32	pH 7.0 PBS	5.0×10^{-7}	[37]
EP			0.16		5.0×10^{-6}	
Serotonin	f-MWCNTs/BR9	DPV	0.21	pH 7.0 PBS	9.0×10^{-6}	Present study
EP			0.16		7.0×10^{-6}	

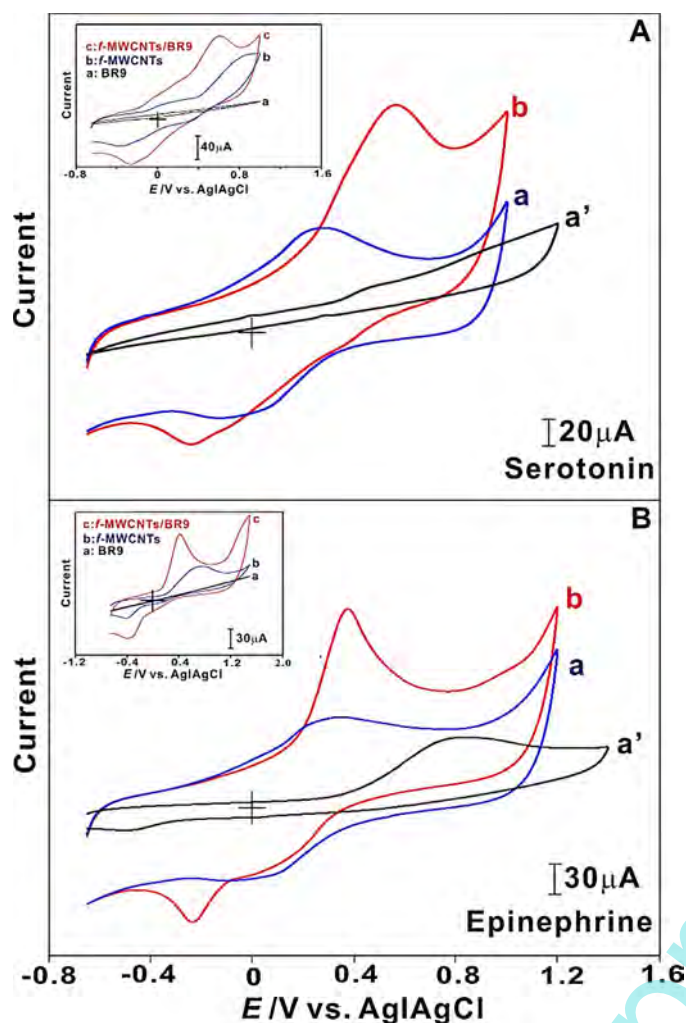SWAV: Square wave anodic stripping voltammograms, SWV: square wave voltammetry

Fig. 5. Cyclic voltammograms of (A) serotonin and (B) epinephrine (EP) at *f*-MWCNTs/BR9 at a scan rate of 100 mV s^{-1}. In all of the sections of (a) *f*-MWCNTs/BR9 in pH 7.0 PBS, (a′) bare GCE and (b) *f*-MWCNTs/BR9 both at serotonin (5 mM) and epinephrine (2.67 mM). The inset displays (a) only BR9, (b) *f*-MWCNTs and (c) *f*-MWCNTs/BR9 at the highest concentrations of analytes.

values exhibited higher efficiency of the *f*-MWCNTs/BR9 film toward the analytes when compared to only *f*-MWCNTs and BR9 films. The *f*-MWCNTs/BR9 film successfully exhibits two well separated electro-oxidation peaks for the detection of serotonin and EP. The peak separation is sufficient for the selective determination of the mixture. The oxidation peaks of serotonin shifted from 331 mV to 211 mV, and the EP peaks shifted from 172 mV to 116 mV (Table 2). For comparison, similar experiments were conducted using modified electrodes, but the response was far from useful for analytical applications.

3.8. Determination of real sample serotonin and epinephrine

DPV of the electrocatalytical values were obtained for serotonin and EP injections in pH 7.0 normal saline (0.9%). Serotonin was prepared in bovine calf serum (BCS). EP injections were obtained from Adrenalin®. Fig. 7(A) displays the electrocatalytic oxidation of serotonin. The peak currents for serotonin increased linearly with the analyte concentration. BCS is similar to human body conditions. Fig. 7(B) displays the electrocatalytic oxidation of the EP injection. The injection labeled composition was 1 mg mL^{-1} EP HCl. In these experiments, the concentration added and found and the relative standard deviation (RSD) were 3–5. From these results, the
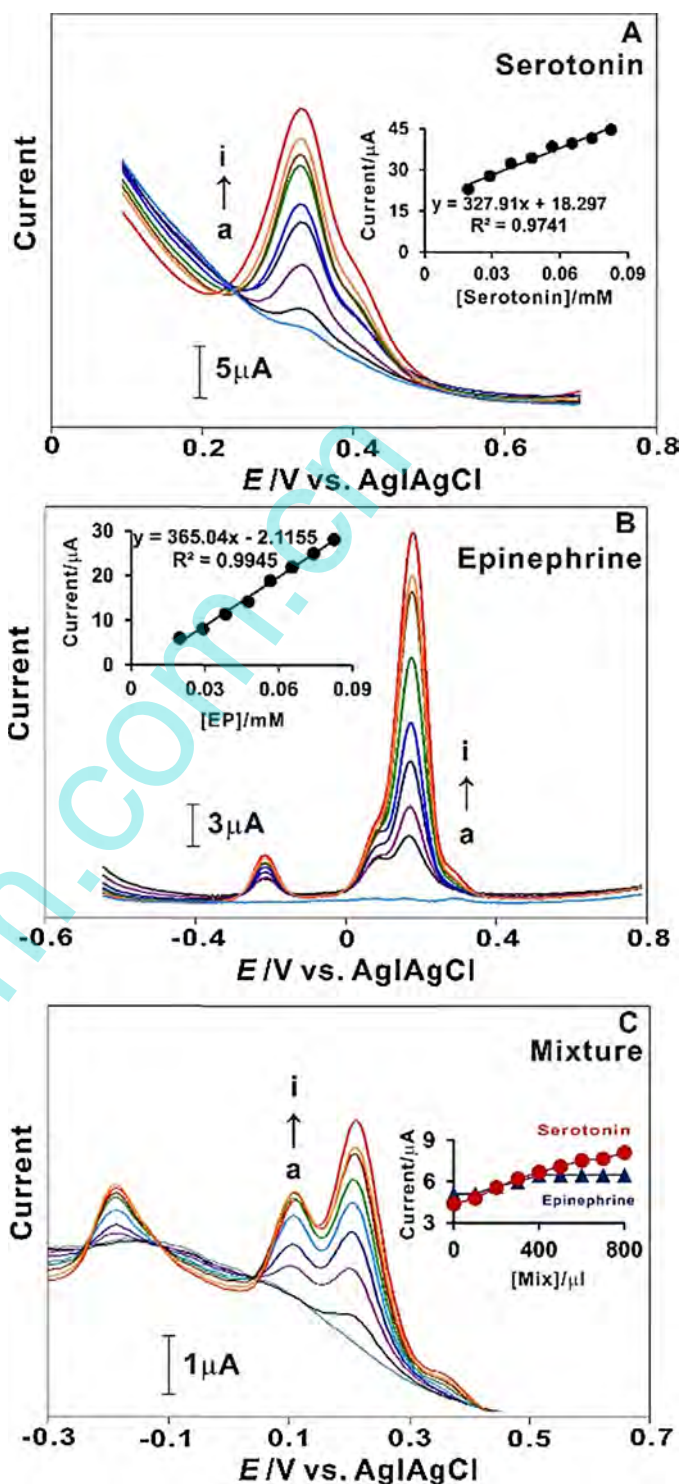

Fig. 6. Differential pulse voltammograms (DPV) of (A) serotonin and (B) epinephrine (EP) at *f*-MWCNTs/BR9 film in various concentrations of: (a) 0; (b) 1.96×10^{-5} M; (c) 2.91×10^{-5} M; (d) 3.84×10^{-5} M; (e) 4.76×10^{-5} M; (f) 5.66×10^{-5} M; (g) 6.54×10^{-5} M; (h) 7.41×10^{-5} M; and (i) 8.25×10^{-5} M. The inset displays the plot of the current versus concentration of serotonin and EP. (C) Simultaneous change in the concentrations of the analyte mixture (serotonin 1.0×10^{-4} M and epinephrine 1.0×10^{-3} M) at the *f*-MWCNTs/BR9 film: (a) 0 μL, (b) 100 μL, (c) 200 μL, (d) 300 μL, (e) 400 μL, (f) 500 μL, (g) 600 μL, (h) 700 μL, and (i) 800 μL in pH 7.0 PBS.

recovery of serotonin was ≈103% and EP was ≈106%. The interference of AA and UA during EP and serotonin determination has been studied using linear sweep voltammetry (LSV). In these experiments, AA and UA maintained high concentrations (5 mM), and
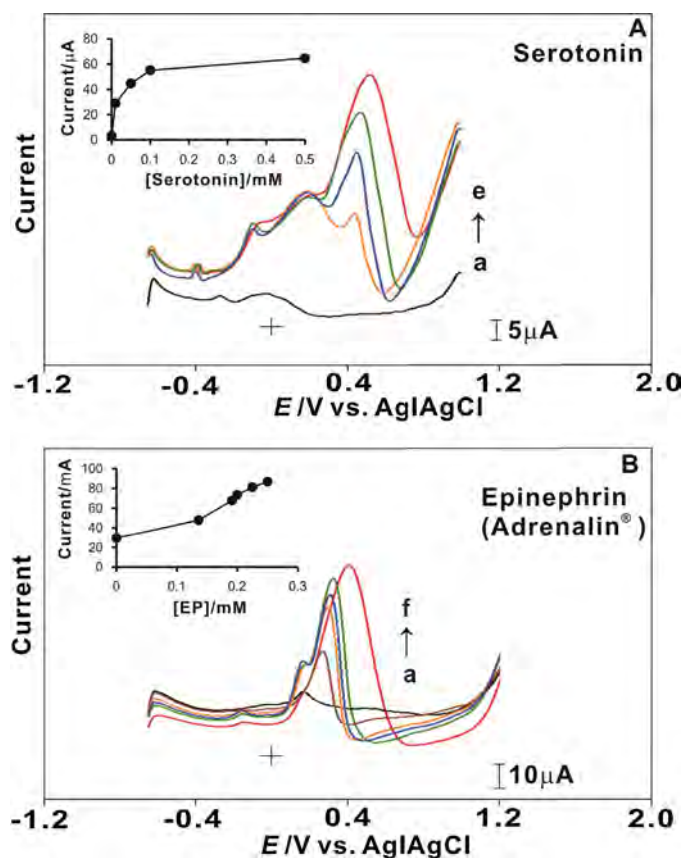
Fig. 7. Differential pulse voltammograms (DPV) of the electrocatalytic values obtained for the serotonin (A) and epinephrine injection (B) determination in pH 7.0 normal saline (0.9%) at the *f*-MWCNTs/BR9 film. The inset displays the plot of the current versus concentration of serotonin and EP.

the concentrations of the EP injections in pH 7.0 normal saline (0.9%) and serotonin in BCS increased from 0.65 mM to 2.67 mM and 0.1 mM to 5 mM. The results reveal that there is no obvious change in the ascorbic acid (AA) and uric acid (UA) current peaks during the addition of EP and serotonin. The above results reveal that *f*-MWCNTs/BR9 composite films could be used for the efficient determination of simple neurotransmitter sensors (Fig. 7).

4. Conclusions

We demonstrated the application of *f*-MWCNTs/BR9 film for the determination of serotonin and EP. Repetitive redox cycling experiments were performed to determine the stability of *f*-MWCNTs/BR9 films in 0.1 M PBS (pH 7.0). This investigation revealed that after 100 continuous scan cycles at a scan rate of 0.1 V s^{-1}, the peak heights of the cyclic voltammograms decreased less than 3%. The *f*-MWCNTs/BR9 film maintained its initial activity for more than 4 weeks when stored in 0.1 M PBS (pH 7.0). A decrease of 6% was observed in the current response of the electrode after 30 days. This feature provides a favorable clinical diagnosis for the electrocatalytic oxidation of serotonin and EP at *f*-MWCNTs/BR9 film.

High sensitivity and excellent stability were demonstrated by the *f*-MWCNTs/BR9 film for neurotransmitter sensing. The SEM and AFM results show the difference between the BR9 and *f*-MWCNTs/BR9 films morphological data. The experimental methods of CVs and DPV were performed with the film biosensors integrated into GCE and ITO. The methods presented in this paper provide an opportunity for qualitative and quantitative characterization, even at physiologically relevant conditions. Therefore, this study establishes and illustrates, in principle and potential, a simple and novel approach for the development of a voltammetric sensor, which is based on the GCE and ITO electrodes.

References

[1] O. Duman, S. Tunc, B. Kancı, Fluid Phase Equilib. 301 (2011) 56.
[2] A.Ş. Koparal, Y. Yavuz, C. Gürel, Ü.L. Öğütveren, J. Hazard. Mater. 145 (2007) 100.
[3] H. Tanaka, H. Katsuura, S. Torii, Electrochim. Acta 42 (1997) 2019.
[4] S.M. Chen, G.H. Chuang, J. Electroanal. Chem. 575 (2005) 125.
[5] U. Yogeswaran, S.M. Chen, J. Electrochem. Soc. 154 (2007) E178.
[6] U. Yogeswaran, S.M. Chen, Sens. Actuators, B 130 (2008) 739.
[7] C. Tang, U. Yogeswaran, S.M. Chen, Anal. Chim. Acta 636 (2009) 19.
[8] Y.Z. Zhou, L.J. Zhang, S.L. Chen, Chin. Chem. Lett. 20 (2009) 217.
[9] U. Yogeswaran, S. Thiagarajan, S.M. Chen, Anal. Biochem. 365 (2007) 122.
[10] M.E.E. Kommos, F.A. Mohamed, A.S.K. Khedr, J. Assoc. Off. Anal. Chem. 73 (1990) 516.
[11] M.H. Sorouraddin, J.L. Manzoori, E. Kargarzadeh, A.M.H. Shabani, J. Pharm. Biomed. Anal. 18 (1998) 877.
[12] M.M. Ardakani, H. Beitollahi, B. Ganjipour, H. Naeimi, Int. J. Electrochem. Sci. 5 (2010) 531.
[13] D.D. Lam, A.S. Garfield, O.J. Marston, J. Shaw, L.K. Heisler, Pharmacol. Biochem. Behav. 97 (2010) 84.
[14] U. Yogeswaran, Y. Li, S.M. Chen, J. Electrochem. Soc. 157 (2010) K187.
[15] M.C. Buhot, S. Martin, L. Segu, Ann. Med. 32 (2000) 210.
[16] A. Meneses, Drug News Perspect. 14 (2001) 396.
[17] G.P. Garcia, A. Meneses, Behav. Brain Res. 195 (2008) 17.
[18] M.A. Dayton, A.G. Ewing, R.M. Wightman, Anal. Chem. 52 (1980) 2392.
[19] J. Chen, C.S. Cha, J. Electroanal. Chem. 463 (1999) 93.
[20] P. Ramesh, G.S. Suresh, S. Sampath, J. Electroanal. Chem. 561 (2001) 173.
[21] Z. Yang, G. Hu, X. Chen, J. Zhao, G. Zhao, Colloids Surf., B: Biointerfaces 54 (2007) 230.
[22] K. Pihel, T.J. Schroeder, R.M. Wightman, Anal. Chem. 66 (1994) 4532.
[23] R.N. Goyal, S. Bishnoi, Electrochim. Acta 56 (2011) 2717.
[24] Y. Li, U. Yogeswaran, S.M. Chen, Anal. Biochem. 388 (2009) 288.
[25] K. Jiang, L.S. Schadler, R.W. Siegel, X. Zhang, H. Zhangc, M. Terrones, J. Mater. Chem. 14 (2004) 37.
[26] K.C. Lin, T.H. Tsai, S.M. Chen, Biosens. Bioelectron. 26 (2010) 608.
[27] J. Wang, J. Dai, T. Yarlagadda, Langmuir 21 (2005) 9.
[28] M. Tahhan, V.T. Truong, G.M. Spinks, G.G. Wallace, Smart Mater. Struct. 12 (2003) 626.
[29] T. Komura, G.Y. Niu, T. Yamaguchi, M. Asano, A. Matsuda, Electroanalysis 16 (2004) 1791.
[30] U. Yogeswaran, S. Thiagarajan, S.M. Chen, Carbon 45 (2007) 2783.
[31] C. Barbero, M.C. Miras, R. Kotz, O. Hass, J. Electroanal. Chem. 437 (1997) 191.
[32] E.P. Kovalchuk, S. Whittingham, O.M. Skolozdra, P.Y. Zavalij, I.Y. Zavaliy, O.V. Reshetnyak, M. Seledets, Mater. Chem. Phys. 69 (2001) 154.
[33] C.P. Andrieux, O. Haas, J.M. SavGant, J. Am. Chem. Soc. 108 (1986) 8175.
[34] F. Wang, Y.Y. Wu, K. Lu, B.X. Ye, Electrochim. Acta 87 (2013) 756.
[35] M.J. Song, S.S. Kim, N.K. Min, J.H. Jin, Biosens. Bioelectron. 52 (2014) 411.
[36] F. Valentini, D. Romanazzo, M. Carbone, G. Palleschi, Electroanalysis 24 (2012) 872.
[37] X.H. Wei, F. Wang, Y.M. Yin, Q.Y. Liu, L.N. Zou, B.X. Ye, Analyst 135 (2010) 2286.